



**HAL**  
open science

## Non-Conventional Features of Plant Oil-Based Acrylic Monomers in Emulsion Polymerization

Ananiy Kohut, Stanislav Voronov, Zoriana Demchuk, Vasylyna Kirianchuk, Kyle Kingsley, Oleg Shevchuk, Sylvain Caillol, Andriy Voronov

► **To cite this version:**

Ananiy Kohut, Stanislav Voronov, Zoriana Demchuk, Vasylyna Kirianchuk, Kyle Kingsley, et al.. Non-Conventional Features of Plant Oil-Based Acrylic Monomers in Emulsion Polymerization. *Molecules*, 2020, 25 (13), pp.2990. 10.3390/molecules25132990 . hal-02885847

**HAL Id: hal-02885847**

**<https://hal.science/hal-02885847>**

Submitted on 1 Jul 2020

**HAL** is a multi-disciplinary open access archive for the deposit and dissemination of scientific research documents, whether they are published or not. The documents may come from teaching and research institutions in France or abroad, or from public or private research centers.

L'archive ouverte pluridisciplinaire **HAL**, est destinée au dépôt et à la diffusion de documents scientifiques de niveau recherche, publiés ou non, émanant des établissements d'enseignement et de recherche français ou étrangers, des laboratoires publics ou privés.

1 Review

## 2 Non-Conventional Features of Plant Oil-Based 3 Acrylic Monomers in Emulsion Polymerization

4 Ananiy Kohut<sup>1</sup>, Stanislav Voronov<sup>1</sup>, Zoriana Demchuk<sup>2</sup>, Vasylyna Kirianchuk<sup>1</sup>, Kyle Kingsley<sup>2</sup>,  
5 Oleg Shevchuk<sup>1</sup>, Sylvain Caillol<sup>3</sup> and Andriy Voronov<sup>2,\*</sup>

6 <sup>1</sup> Department of Organic Chemistry, Institute of Chemistry and Chemical Technologies, Lviv Polytechnic  
7 National University, Lviv, Ukraine; ananiy.kohut@gmail.com (A.K.); stanislav.voronov@gmail.com (S.V.);  
8 vasuluna411@ukr.net (V.K.); oshev2509@gmail.com (O.S.)

9 <sup>2</sup> Department of Coatings and Polymeric Materials, North Dakota State University, Fargo, ND, United States;  
10 zoriana.demchuk@ndsu.edu (Z.D.); kyle.kingsley.2@ndsu.edu (K.K.); andriy.voronov@ndsu.edu (A.V.)

11 <sup>3</sup> ICGM, Univ Montpellier, CNRS, ENSCM, Montpellier, France, sylvain.caillol@enscm.fr (S.C.)

12 \* Correspondence: andriy.voronov@ndsu.edu

13 Received: date; Accepted: date; Published: date

14 **Abstract:** In recent years, polymer chemistry has experienced an intensive development of a new  
15 field regarding the synthesis of aliphatic and aromatic biobased monomers from renewable plant  
16 sources. A one-step process for the synthesis of new vinyl monomers by the reaction of direct  
17 transesterification of plant oil triglycerides with N-(hydroxyethyl)acrylamide has been recently  
18 invented to yield plant oil-based monomers (POBMs). The features of the POBM chemical  
19 structure, containing both a polar (hydrophilic) fragment capable of electrostatic interactions, and  
20 hydrophobic acyl fatty acid moieties (C15-C17) capable of van der Waals interactions, ensures the  
21 participation of the POBMs fragments of polymers in intermolecular interactions before and during  
22 polymerization. The use of the POBMs with different unsaturations in copolymerization reactions  
23 with conventional vinyl monomers allows for obtaining copolymers with enhanced  
24 hydrophobicity, provides a mechanism of internal plasticization and control of crosslinking degree.  
25 Synthesized latexes and latex polymers are promising candidates for the formation of hydrophobic  
26 polymer coatings with controlled physical and mechanical properties through the targeted control  
27 of the content of different POBM units with different unsaturations in the latex polymers.

28 **Keywords:** Biobased polymers; plant oil-based monomers; mixed micelles; methyl- $\beta$ -cyclodextrin  
29 inclusion complex; emulsion polymerization.

### 31 1. Introduction

32 The problem of depletion of fossil raw materials has become of global importance and is  
33 complicated not only by economic but also environmental and political factors [1]. However,  
34 synthetic polymers are still one of the most widely used materials in everyday use. Environmental  
35 analysis shows that huge amounts of plastic waste are found in the environment, and their  
36 contribution to the ever-increasing amount of solid waste is a significant environmental threat [2].  
37 Plant oils are low-cost raw materials for the manufacture of monomers and polymers [3-5], which  
38 have several advantages over conventional polymeric materials, namely biodegradability,  
39 non-toxicity, biocompatibility, and hydrophobicity. Therefore, an important task for synthetic  
40 chemists is to consider renewable raw materials as an alternative to raw counterparts of fossil origin.  
41 Due to the wide range of plant oils, the variety of their chemical compositions, and, in many cases,  
42 abandon of resources, they became an interesting object to be used in polymers synthesis as a  
43 renewable raw material.

44 The total production of plant oils in the world in 2019 amounted to more than 200 million tons,  
 45 of which about 15% are used as raw materials for the synthesis of new chemical compounds and  
 46 materials [6]. The presence of plant oils or their derivatives (fatty acids) in various compositions of  
 47 polymeric materials improves their optical (gloss), physical (flexibility, adhesion) [7,8], and chemical  
 48 (resistance to water and chemicals) properties [9]. The synthesis of biobased monomers from  
 49 renewable resources is a promising platform for the synthesis and implementation of new  
 50 environmentally friendly industrial polymer materials [10]. It should be noted that methods for the  
 51 synthesis of vinyl monomers based on soybean, olive, and linseed oils through plant oil direct  
 52 transesterification with N-(hydroxyethyl)acrylamide [10-12] has been recently developed along with  
 53 methods of their copolymerization [13]. The ability of these plant oil-based monomers (POBMs) to  
 54 undergo free radical (co)polymerization reactions has been confirmed and demonstrated [11,13,14].  
 55 The conversion, polymerization rate, and molecular weight of the polymers have been shown to  
 56 depend on unsaturation of the plant oil chosen for POBMs synthesis [11,13].

## 57 2. Features of Synthesis of Vinyl Monomers from Plant Oils

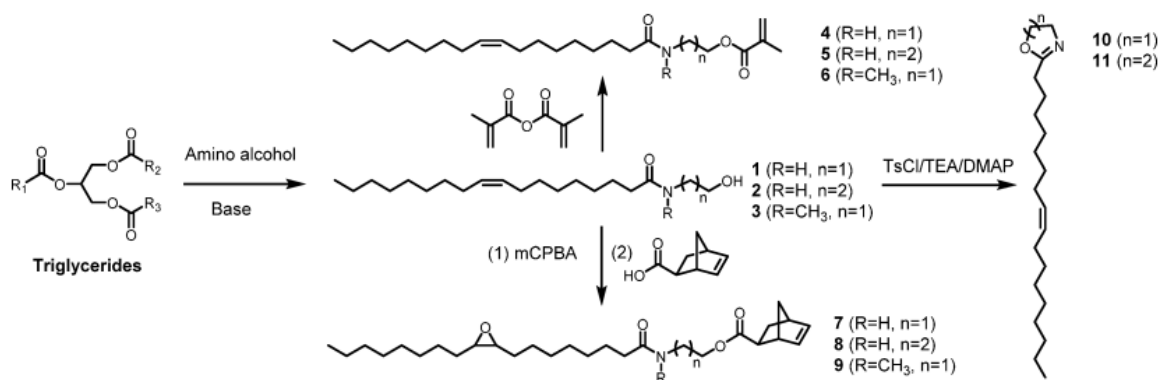
58 Harrison and Wheeler have shown for the first time [15] that the polymerization rate decreases  
 59 with increasing unsaturation degree of acrylates containing acyl moieties of unsaturated fatty acids.  
 60 They explained that the retarding of the polymerization rate and the low conversion are due to the  
 61 interaction of radicals with the mobile hydrogen atoms in the acyl moieties. This leads to the  
 62 formation of new allylic radicals of low activity which retards propagation of polymer chains (chain  
 63 transfer reaction, retardation of the process) [15].

64 Through the esterification reaction of fatty alcohols with acryloyl chloride, Chen and Bufkin  
 65 synthesized a range of acrylates, including linoleyl acrylate, oleyl acrylate, and lauryl acrylate, and  
 66 studied their copolymerizability. They showed that the presence of fatty fragments in acrylate  
 67 molecules determines their polarity, which leads to alternating copolymerization with methyl  
 68 methacrylate [16].

69 In their next study [17], Chen and Bufkin confirmed the results of Harrison's research [15] and  
 70 showed that the presence of fatty acid moieties in the structure of the new acrylates leads to a  
 71 decrease in both the polymerization rate and polymer molecular weights because of chain transfer  
 72 reactions. Increasing the content of unsaturated acyl groups in the copolymer also reduces its glass  
 73 transition temperature. The authors suggested the mechanisms for crosslinking acrylate copolymers  
 74 and studied their physical and mechanical properties [17].

75 Through amidation of triglycerides with amino alcohols, natural derivatives of surfactants and  
 76 lubricants were obtained [18].

77 Tang et al. [19] reported on the synthesis of N-hydroxyalkylamides and methacrylate  
 78 hydrophobic monomers through the interaction of plant oil triglycerides with amino alcohols  
 79 (Figure 1). They developed a new interesting approach that involves the use of a two-step process. In  
 80 the first stage, the interaction of triglycerides with amino alcohols with the formation of  
 81 N-hydroxyalkylamides by the amidation reaction:



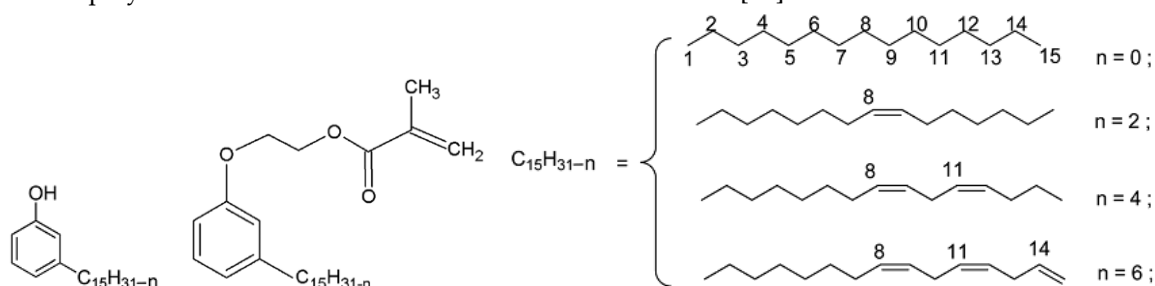
82 **Figure 1.** Transformation of triglycerides in N-hydroxyalkylamides and methacrylate monomers.  
 83 Reprinted with permission from [19]. Copyright (2015) American Chemical Society.

84 Aminoalcohols, namely ethanolamine (R = H, n = 1), 3-amino-1-propanol (R = H, n = 2), and  
 85 N-methylethanolamine (R = CH<sub>3</sub>, n = 1), were used as chemicals which enables the synthesis of a  
 86 wide range of new monomers. In the second stage, the corresponding monomers were synthesized  
 87 by the interaction between N-hydroxyethylamides R'-C(O)-N(R)-(CH<sub>2</sub>)<sub>n</sub>-CH<sub>2</sub>OH and methacrylic  
 88 anhydride. In such a way, methacrylate monomer based on high oleic soybean oil was synthesized:



90 A study of free radical polymerization of these monomers revealed that the double bonds in the  
 91 fatty acid chains remain unaffected during the reaction. The synthesized methacrylate monomers  
 92 based on high oleic soybean oil, depending on the nature of the branches in the side chain, have a  
 93 wide range of glass transition temperatures [19]. In further studies, Tang and co-authors used more  
 94 than twenty amino alcohols to establish the mechanism of amidation of plant oils, in particular  
 95 high-oleic soybean oil [8]. Depending on the nature of the acyl fatty acid and amide structures, the  
 96 polymers have a wide range of glass transition temperatures – from viscoelastic to thermoplastic  
 97 materials. The possibility of controlled hydrogenation of unsaturated double bonds was also shown,  
 98 which provides control over thermal and mechanical properties of polymers [8].

99 It was demonstrated that the high reactivity of the vinyl group of the acrylate monomers based  
 100 on plant oils determines the course of their polymerization and copolymerization by a free radical  
 101 mechanism [20]. Caillol et al. [21,22] proposed methods for the synthesis of a new monomer from  
 102 cardanol (Figure 2), which is isolated from cashew nuts. Reactivity of the cardanol-based monomer  
 103 in the copolymerization reactions with the POBMs was studied [23].



104

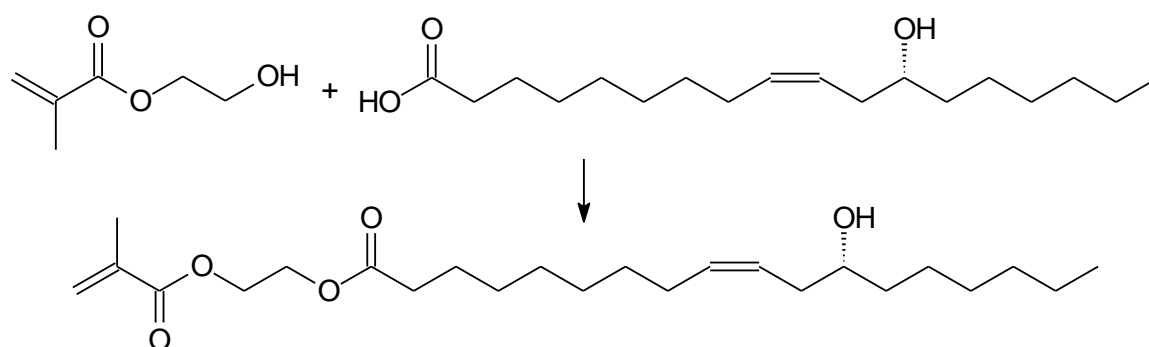
105 **Figure 2.** Structure of cardanol and a cardanol-based monomer. Adapted from Ref. 21 with  
 106 permission from The Royal Society of Chemistry.

107 Cardanol-based polymers have a controlled flexibility due to "internal plasticization", which  
 108 occurs due to the presence of a long side chain. The presence of these fragments also provides  
 109 polymeric materials based on cardanol with hydrophobic properties. It should be noted that  
 110 cardanol exhibits antimicrobial and anti-termite properties and, under certain conditions, can  
 111 provide them to copolymers based on it. It is compatible with a wide range of polymers, such as  
 112 alkyds, melamines, polyesters, *etc.* [21].

113 In the study [22], synthetic pathways to molecular blocks from cardanol by one- or two-stage  
 114 methods were reported. In particular: 1) dimerization/oligomerization of cardanol, to increase its  
 115 functionality; 2) synthesis of reactive amines by thiol-ene coupling; 3) epoxidation and  
 116 (meth)acrylation of cardanol for the synthesis of polymers and materials with oxirane or  
 117 (meth)acrylate groups.

118 A feature of cardanol-based monomers and polymers is the presence of aromatic fragments and  
 119 fatty moieties in their structure at the same time. The authors showed that cardanol-based polymeric  
 120 materials have prospective properties for manufacturing coatings, in particular, with enhanced  
 121 mechanical and thermal properties [22].

122 Recently, methacrylated ricinoleic acid monomer (Figure 3) was synthesized by the  
 123 esterification reaction of ricinoleic acid with 2-hydroxyethyl methacrylate [24]:

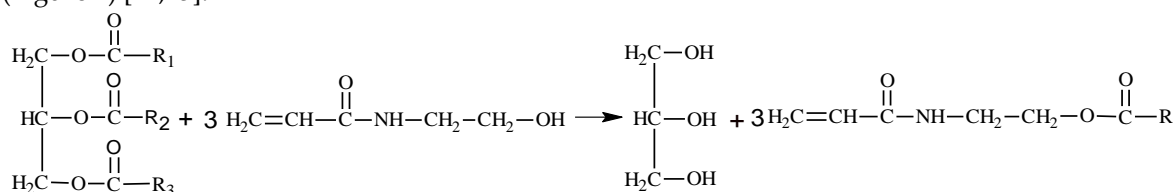


124  
125

**Figure 3.** Schematic of synthesis of methacrylated ricinoleic acid monomer [24].

126 It should be noted that all known methods for the synthesis of monomers from plant oil  
127 triglycerides are multi-stage and involve several steps, which makes their implementation in  
128 industry more challenging.

129 Recently, we developed a one-step process for the synthesis of new vinyl monomers by the  
130 direct transesterification reaction of plant oil triglycerides with N-(hydroxyethyl)acrylamide  
131 (Figure 4) [12,25].



132  
133  
134  
135

**Figure 4.** Schematic of synthesis of acrylic monomers based on plant oil triglycerides where  $R_1$ ,  $R_2$ ,  $R_3$  are saturated and unsaturated fatty acid chains with one or several double bonds. Reprinted with permission from [10]. Copyright (2015) American Chemical Society.

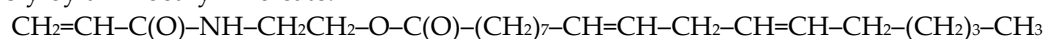
136 Using this process, a range of plant oil-based monomers – POBMs was synthesized by the direct  
137 transesterification reaction between N-(hydroxyethyl)acrylamide and plant oil triglycerides  
138 (Figure 4) [10,11]. In the reaction, N-(hydroxyethyl)acrylamide can be considered as an alcohol  
139 ROH – where the unsaturated fragment  $\text{CH}_2=\text{CH}-\text{C}(\text{O})-\text{NH}-\text{CH}_2-\text{CH}_2-$  is a residue  $-\text{R}$ . Upon the  
140 alcoholysis (transesterification), a residue exchange between the triglyceride and N-(hydroxyethyl)-  
141 acrylamide occurs leading to formation of the corresponding monomers.

142 The POBMs synthesis was conducted in THF with an excess of N-(hydroxyethyl)acrylamide  
143 (molar ratio of N-hydroxyethylacrylamide to triglyceride as 5.9: 1) in order to achieve complete  
144 transesterification of the triglycerides. The yield of the desired monomers was about 94-96%. The  
145 reaction by-product (glycerol) and the excessive (N-hydroxyethyl)acrylamide are easily removed by  
146 washing with brine after diluting the reaction mixtures with  $\text{CH}_2\text{Cl}_2$ . The POBMs sparingly soluble  
147 in water remain in the organic phase. To avoid free radical polymerization, 2,6-di-*tert*-butyl-p-cresol  
148 (0.05 to 0.1% by weight) was added as an inhibitor to the reaction mixtures prior the synthesis.

149 Upon the alcoholysis of olive oil with N-(hydroxyethyl)acrylamide, 2-N-acryloylaminoethyl  
150 oleate is predominantly formed:

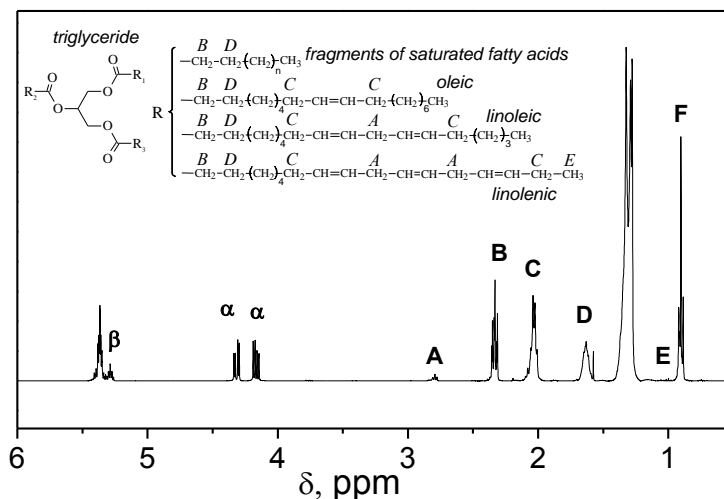


151 This monomer contains one double bond in the acryloylamide moiety and one double bond in  
152 the fatty acid chain. Such a structure, in comparison with the soybean oil-based monomer –  
153 2-N-acryloylaminoethyl linoleate:



154 reduces the extent of the chain transfer reaction. Accordingly, fewer less active radicals are formed  
155 and the polymerization reaction proceeds to higher conversion with a less pronounced retardation  
156 effect. This leads to the formation of polymers (copolymers) with a higher molecular weight and a  
157 lower polydispersity index.  
158  
159

160 The composition of plant oils is known to depend on the type of crop raw material. Therefore,  
 161 an important step was to determine the content of different fatty acid chains in the mixture of  
 162 monomers obtained upon the transesterification of olive oil with N-(hydroxyethyl)acrylamide. The  
 163 content of fatty acid chains in the oil was determined from the integral intensities of the  
 164 characteristic proton signals of each fatty acid chain and glycerol fragments using  $^1\text{H}$  NMR  
 165 spectroscopy of the plant oil [26] (Figure 5).



166

167 **Figure 5.**  $^1\text{H}$  NMR spectrum of olive oil. Adapted with permission from [11]. Copyright (2016)  
 168 American Chemical Society.

169 The content of the linolenic acid units (linolenate) in olive oil was calculated by measuring the  
 170 integral value of the signal at 1 ppm, which corresponds to the protons of the methyl group in a  
 171 linolenic acid chain (signal E in Figure 5). Taking into account only one of the signals of  $\alpha$ -protons of  
 172 glycerol, *i.e.* the signal at 4.27 ppm (Figure 5), the ratio of the integral values is two  $\alpha$ -glycerol  
 173 protons to three protons of the linolenic acid methyl group. It should be kept in mind that three  
 174 linolenic acid chains can undergo transesterification in the same glycerol molecule. A field correction  
 175 factor is the ratio of two protons of glycerol to nine protons of the linolenic acid methyl groups. By  
 176 converting the ratio of these areas to percentages, a ratio of 22.2% glycerol to 100% linolenic acid was  
 177 obtained [26]. Calibration of the integral value of one of the glycerol  $\alpha$ -proton signals to the value in  
 178 the  $^1\text{H}$  NMR spectrum in the signal region at 0.98 ppm directly gives the percentage of linolenic acid  
 179 in the sample – 0.73%.

180 The percentage of linoleic acid chains (linoleates) in olive oil was determined from the ratio of  
 181 the integral value of the signal at ~2.74 ppm, which corresponds to the methylene protons between  
 182 two double bonds (signal A in Figure 5), to the integral value of one of glycerol  $\alpha$ -protons. The field  
 183 correction factor (33.3) is the ratio of two glycerol protons to six possible methylene protons in  
 184 linoleate. The amount of linoleic acid is calculated by subtracting the twiced content of linolenic acid,  
 185 determined from the peak at 2.74 ppm [26].

186 The percentage of oleic acid chains (oleates) was determined from the ratio of the integral value  
 187 of the signal at ~2.02 ppm, which corresponds to the protons in the  $\alpha$ -position to the double bond of  
 188 all unsaturated fatty acids (signal C in Figure 5), to the integral value of one of glycerol  $\alpha$ -protons.  
 189 Accordingly, the ratio of two glycerol protons to twelve possible protons in the  $\alpha$ -position to the  
 190 double bond of all unsaturated fatty acids is the field correction factor equal to 16.7. The percentage  
 191 of oleic acid was calculated by subtracting the content of unsaturated linolenic and linoleic acid  
 192 chains from the determined value [26].

193 The content of saturated fatty acid chains was determined from the fact that the total content of  
 194 fatty acids is 100%, and the amount of unsaturated fatty acid chains was subtracted from 100%. The  
 195 determined content of fatty acid chains is given in Table 1. These data are in a good agreement with  
 196 the literature data obtained by gas chromatography of olive oil [27].

197 Thus, according to  $^1\text{H}$  NMR spectroscopy, the olive oil triglycerides include: saturated fatty acid  
 198 chains (C18:0) – 12.44%; oleic acid chains (C18:1) – 80.23%; linoleic acid chains (C18:2) – 6.60%; and  
 199 linolenic acid chains (C18:3) – 0.73%.

200 **Table 1.** Content of fatty acid chains in olive oil.

Fatty acid chains	Signal (protons)	Field correction factor		Content of fatty acids in the oil, %	
			%	Calculated	Literature data
linolenate (E)	0.95-1.05 ppm (-CH <sub>3</sub> )	2H/9H	22.2	<b>0.73</b>	< 1 %
linoleate (A)	2.75-2.85 ppm (-CH=CH-CH <sub>2</sub> -CH=CH-)	2H/6H	33.3	8.06 - 2·0.73 = <b>6.6</b>	3.5-21
oleate (C)	1.97-2.11 ppm (-CH <sub>2</sub> -CH=CH-CH <sub>2</sub> -)	2H/12H	16.7	87.56-(0.73+6.6)= <b>80.23</b>	55-83 %
Content of saturated fatty acid chains:				100-(0.73+6.6+80.23)= <b>12.44</b>	1-20 %

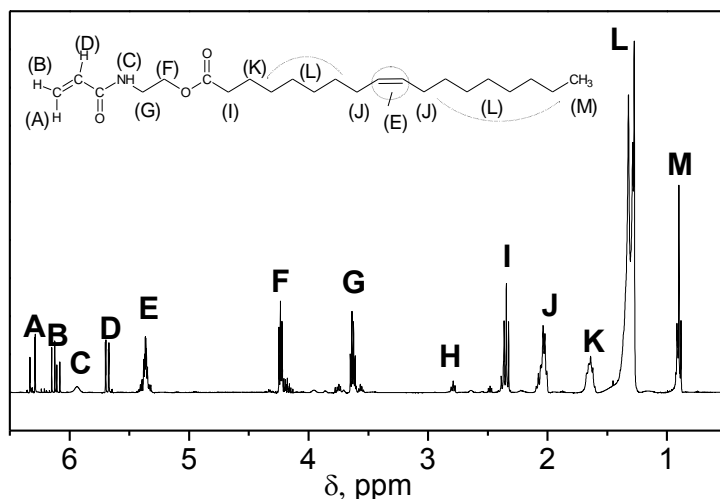
201 These results are consistent with the literature data obtained by gas chromatography of olive  
 202 oil, where the saturated chains make up 1-20%, oleic acid chains 55-83%, linoleic acid chains 3.5-21%,  
 203 and linolenic acid chains less than 1% [28]. Using this approach, monomers based on various plant  
 204 oils were successfully synthesized and characterized (Table 2).

205 **Table 2.** Physico-chemical characteristics of POBMs.

Monomer from Oil	Content of unsaturated fatty acids, %			Iodine value (same for oil), g/g	Molar mass, g/mol
	C <sub>18:1</sub>	C <sub>18:2</sub>	C <sub>18:3</sub>		
High Oleic Sunflower Oil (HOSFM)	86-89	3-6	0.5-1	105 (82)	379.0 <sup>1</sup>
Olive Oil (OVM)	65-85	3.5-20	0-1.5	110 (90)	379.3 <sup>2</sup>
High Oleic Soybean Oil (HOSBM)	70-73	13-16	0-1	124(105)	379.3 <sup>2</sup>
Canola Oil (CLM)	60-63	18-20	8-10	137 (96)	379.0 <sup>2</sup>
Corn Oil (COBM)	23-31	49-62	0-2	139 (120)	377.0 <sup>1</sup>
Sunflower Oil (SFM)	14-35	44-75	0-1	146 (128)	377.5 <sup>2</sup>
Soybean Oil (SBM)	22-34	43-56	7-10	149 (139)	377.3 <sup>2</sup>
Linseed Oil (LSM)	12-34	17-24	35-60	194 (177)	375.6 <sup>1</sup>

206 <sup>1</sup>Calculated.<sup>2</sup>Experimental.

207 The monomer structure was confirmed by FTIR and  $^1\text{H}$  NMR spectroscopy [11]. A  $^1\text{H}$  NMR  
 208 spectrum of the olive oil-based monomer is shown in Figure 6 where the characteristic peaks at  
 209 6.6 ppm indicate the presence of an acryloylamide moiety (protons of the acrylic double bond)  
 210 whereas the peaks at 3.6 and 4.2 ppm correspond to the protons of two methylene groups between  
 211 the amide and ester groups. Similar spectra are recorded for other POBMs, which confirms the  
 212 presence of the similar acryloylamide moiety (protons of the vinyl double bond) in their molecules.  
 213 This allows for predicting similar reactivity of the vinyl group in the monomers acryloylamide  
 214 moiety in the radical polymerization [11].



215

216

217

**Figure 6.**  $^1\text{H}$  NMR spectrum of the olive oil-based monomer. Adapted with permission from [11]. Copyright (2016) American Chemical Society.

218

219

220

221

222

The peaks in the range from 0.8 to 2.8 ppm correspond to the fatty acid chain protons. The peaks at 5.3 – 5.44 ppm imply the presence of protons at the carbon-carbon double bonds in the fatty acid chain. The peaks at 1.98 – 2.14 ppm indicate the presence of protons in the  $\alpha$ -position to the double bond (allylic hydrogen), capable of the chain transfer reaction and the formation of less active free radicals [11].

223

224

225

226

227

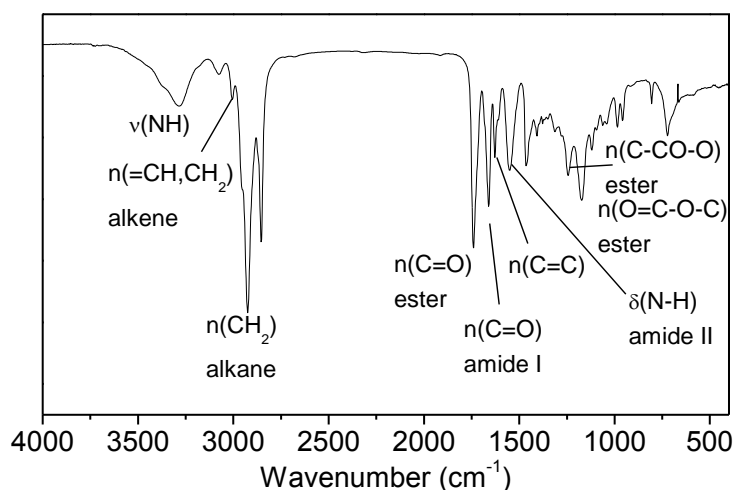
228

229

230

231

According to the FTIR spectroscopy data, the appearance of the strong absorption bands at 3400 – 3200  $\text{cm}^{-1}$  (NH bonds), at 1670  $\text{cm}^{-1}$  (the carbonyl group, amide I), and at 1540  $\text{cm}^{-1}$  (NH, amide II) in the spectra of the POBMs (*e.g.*, the olive monomer – Figure 7) indicates the addition of fatty acid acyl moieties to the acrylamide fragment. The absorption bands at 1740, 1245, and 1180  $\text{cm}^{-1}$  confirm the presence of an ester group in the monomer molecule. The absorption bands at 1665–1635  $\text{cm}^{-1}$  indicate the presence of a carbon-carbon bond double in the fatty acid chains [11]. FTIR spectra of monomers based on other plant oils are pretty similar. Hence, the synthesized POBMs can be attributed to the conventional vinyl monomers because the acryloylamide moiety provides the participation of these monomers in the free radical polymerization.



232

233

234

**Figure 7.** FTIR spectrum of the olive oil-based monomer. Adapted with permission from [11]. Copyright (2016) American Chemical Society.

235

236

237

238

The content of fatty acid chains in the monomer mixture produced by the transesterification of plant oils with N-(hydroxyethyl)acrylamide was determined on the example of the olive monomer by calculating the ratio of the integral values in the  $^1\text{H}$  NMR spectra of the commercial oil and the resulting monomer mixture (Figure 8).

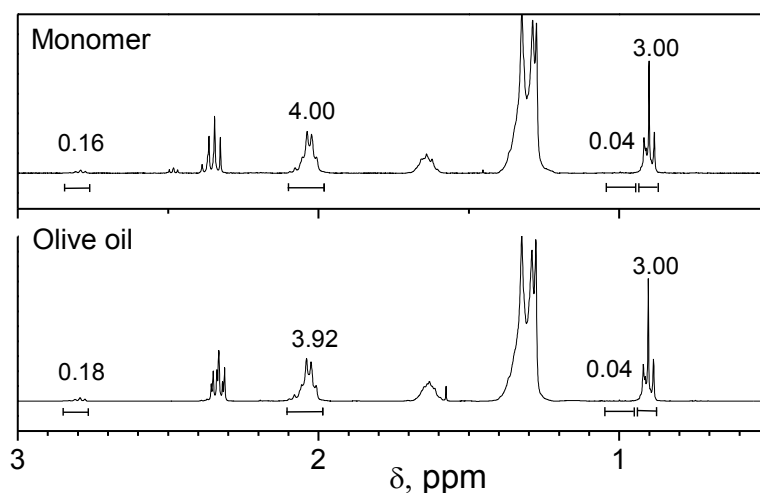


Figure 8.  $^1\text{H}$  NMR spectra of the olive oil and the olive oil-based monomer.

239

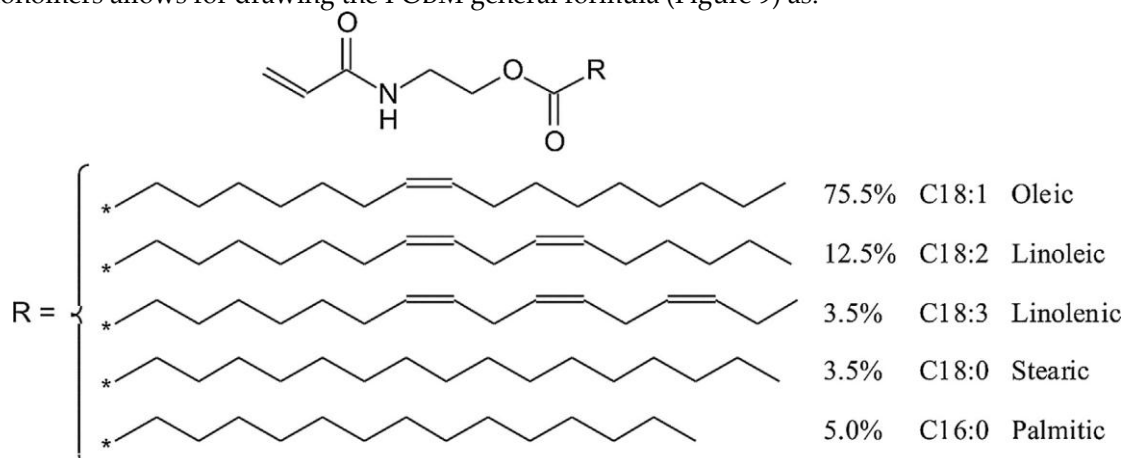
240

241 According to the  $^1\text{H}$  NMR spectroscopy data, the monomer mixture consists of: saturated fatty  
 242 acid chains (C18:0) – 11.47% (stearic and palmitic); oleic acid chains (C18:1) – 81.9%; linoleic acid  
 243 chains (C18:2) – 5.9%; and linolenic acid chains (C18:3) – 0.73% after the olive oil transesterification.

244 Thus, the major component of the olive monomer is a monomer with oleic acid chains (81.9%) –  
 245 2-N-acryloylaminoethyl oleate. The soybean monomer is mainly a monomer with linoleic acid  
 246 chains (57.5%) – 2-N-acryloylaminoethyl linoleate whereas the linseed monomer predominantly  
 247 consists of a monomer with linolenic acid chains (58%) – 2-N-acryloylaminoethyl linolenate.

248 One of the most important characteristics of monomers is the unsaturation degree, which for  
 249 POBMs is determined by the number of the double bonds in the fatty acid chains. To compare the  
 250 monomers in terms of the unsaturation degree, their iodine values were determined and compared  
 251 with those for the corresponding plant oils used for the synthesis of the POBMs (Table 2). The  
 252 obtained results show that the iodine value for the monomers is higher than those for the oils, due  
 253 to the presence of an unsaturated acryloylamide moiety. Depending on the type of oil, the iodine  
 254 values for various monomers differ. For instance, the iodine value for 2-N-acryloylaminoethyl oleate  
 255 (110 g / 100 g) is significantly lower than that for 2-N-acryloylaminoethyl linoleate (149 g / 100 g) due  
 256 to the different unsaturation degree of the molecules. Besides the acryloylamide moiety, there are  
 257 two double bonds in the fatty acid chain of the soybean monomer molecule [10]. The low solubility  
 258 of these monomers in water implies their **highly hydrophobic** nature [11].

259 Analysis of the data obtained from the synthesis and characterization of plant oil-based acrylic  
 260 monomers allows for drawing the POBM general formula (Figure 9) as:



261

262

263

Figure 9. General formula of the plant oil-based monomers. Reprinted from Ref. 35, Copyright (2018), with permission from Elsevier.

### 264 3. Features of Homo- and Copolymerization of Plant Oil-Based Acrylic Monomers

265 The reactivity of the plant oil-based monomers in the free radical polymerization reactions  
266 (chain growth reaction) is determined by the presence of an acryloylamide moiety containing a vinyl  
267 group which is common for all monomers. However, the POBMs contain a certain amount of  
268 unsaturated fatty acid chains of various structure (the different numbers of both double bonds and  
269 hydrogen atoms in the  $\alpha$ -position to the double bonds). This causes the monomers to participate in  
270 chain transfer reactions due to the abstraction of the allylic hydrogen atoms and the formation of less  
271 active radicals. Hence, the monomer chain transfer constants  $C_M$  clearly depend on monomer  
272 structure as follows: 0.033 (most unsaturated LSM) > 0.026 (SBM) > 0.023 (SFM) > 0.015 (least  
273 unsaturated OVM) with respect to decreasing number of C-H groups in the  $\alpha$ -position of the fatty  
274 acid double bonds) [11]. This impacts the polymerization conversion and molecular weights of the  
275 resulting polymers (copolymers) from the POBMs.

276 The features of **homopolymerization** kinetics for 2-N-acryloylaminoethyl oleate revealed that  
277 the orders of reaction with respect to monomer and initiator are 1.06 and 1.2, respectively. The  
278 unsaturation degree of fatty acid chains in the POBM molecules was used as a criterion for  
279 comparing the kinetic data of homopolymerization of 2-N-acryloylaminoethyl oleate and  
280 2-N-acryloylaminoethyl linoleate. The observed deviations of the orders of reaction are due to the  
281 specific mechanism of the homopolymerization reaction of 2-N-acryloylaminoethyl oleate which  
282 includes two simultaneous reactions (chain propagation and transfer) [11]. Although the  
283 propagating radicals might be very reactive, once the chain is transferred to the allylic C-H, the  
284 newly formed radical becomes more stable due to resonance stabilization and does not readily  
285 initiate new chains. In comparison with the soybean monomer, the olive monomer is less involved  
286 into the chain transfer reactions (the chain transfer constant  $C_M = 0.015$  for OVM while for SBM  
287  $C_M = 0.026$ ). As a result, the homopolymerization of the olive monomer occurs at a higher rate of  
288  $12.2 - 45.3 \cdot 10^{-5} \text{ mol}/(\text{L} \cdot \text{s})$  when compared with the more unsaturated soybean monomer -  
289  $4.3 - 11.3 \cdot 10^{-5} \text{ mol}/(\text{L} \cdot \text{s})$ . The molecular weights of the homopolymers were determined by gel  
290 permeation chromatography. The resulting homopolymers from OVM have higher number average  
291 molecular weights and lower polydispersity indexes (16 800–23 200 g/mol for 2-N-acryloylamino-  
292 ethyl oleate compared to 13 600–14 300 g/mol for 2-N-acryloylaminoethyl linoleate).

293 The reactivity of the plant oil-based monomers in chain **copolymerization** was studied in  
294 POBMs reactions with styrene and vinyl acetate. A characteristic feature of the POBMs is the  
295 presence of the acryloylamide fragment ( $\text{CH}_2=\text{CH}-\text{C}(\text{O})-\text{NH}-\text{CH}_2-\text{CH}_2-$ ) in their structure, which  
296 determines the monomer reactivity in copolymerization. The composition of the copolymers was  
297 determined from  $^1\text{H}$  NMR spectroscopy data. Radical copolymerization of the plant oil-based  
298 monomers is described with the classical Mayo–Lewis equation. The Alfrey–Price  $Q$  (0.41–0.51) and  
299  $e$  (0.09–0.28) parameters are close for all POBMs and do not essentially depend on the monomer  
300 structure [13]. This is due to the presence of the same acryloylamide moiety in the POBM molecules  
301 which determines the monomer reactivity in polymerization reactions.

302 The features of copolymerization are determined by the structure of monomers based on plant  
303 oil triglycerides along with the degradative chain transfer by formation of less active radicals.  
304 Nevertheless, the growth of macrochains can be described with the conventional features of chain  
305 copolymerization, yielding copolymers with a potential to be used in a broad variety of applications.

306 Vinyl monomers from plant oils that have different degrees of unsaturation, soybean and olive  
307 oils, were copolymerized in emulsion with styrene to investigate the kinetics features and feasibility  
308 of latex formation. The kinetics of emulsion copolymerization of styrene with the olive and soybean  
309 monomers agree with the Smith-Ewart theory since the number of nucleated latex particles is  
310 proportional to the surfactant and initiator concentration to the powers 0.58–0.64 and 0.39–0.46,  
311 respectively [29]. Copolymerization of styrene with plant oil-based monomers follows the typical  
312 phenomenology for emulsion polymerization of hydrophobic monomers with a micellar nucleation  
313 mechanism. When the POBMs were copolymerized in emulsion with significantly more water  
314 soluble comonomers, methyl methacrylate and vinyl acetate, latex particle nucleation mainly  
315 occurred through homogeneous mode. For the emulsion copolymerization of methyl methacrylate

316 with OVM and SBM, the reaction orders with respect to emulsifier and initiator are 0.33–0.67 and  
317 0.56–0.69, respectively. It was shown that upon adding the highly hydrophobic POBMs into the  
318 monomer mixture, the latex polymer particles originating from micellar nucleation essentially  
319 increases [14].

320 Using emulsion and miniemulsion copolymerization of the olive and soybean monomers with  
321 styrene or methyl methacrylate, stable aqueous dispersions of polymers with latex particle sizes of  
322 40–210 nm were produced. The content of the POBM units in the macromolecules of the latex  
323 polymers is 5–60 wt.%. The average molecular weight of the synthesized polymers varies in the  
324 range of 30 000–391 500. It was found that the molecular weight of the latex copolymers decreases  
325 with increasing unsaturation degree of the POBMs and their content in the reaction mixture, which  
326 is explained by degradative chain transfer to unsaturated fatty acid chains [14,29].

327 An analysis of the literature shows a rapid development of a new branch in polymer science  
328 related to the chemistry of aliphatic and aromatic biobased monomers from renewable plant sources.  
329 The synthesis of such monomers allows for producing fully biobased polymers with biocompatible  
330 and biodegradable properties which do not pollute the environment. Copolymerization of  
331 monomers synthesized from various plant oils, which have different unsaturation, enables  
332 formation of copolymers with side branches of the macrochain with different unsaturation degrees.  
333 A large variety of the POBMs allows to synthesize polymers having moieties with different  
334 unsaturation, and to make coatings with adjustable cross-linking degree thereof, including latex  
335 copolymers from fully biobased monomer mixtures [23]. Remarkably, copolymerization of the  
336 POBMs with commercial vinyl monomers enables synthesis of polymers with enhanced  
337 hydrophobicity along with the mechanism of internal plasticization.

338 Synthesized latex polymers and copolymers are prospective candidates for the formation of  
339 moisture-/water-resistant polymer coatings with controlled physical and mechanical properties  
340 using controlled content of incorporated POBM units with different unsaturation in the latex  
341 structure.

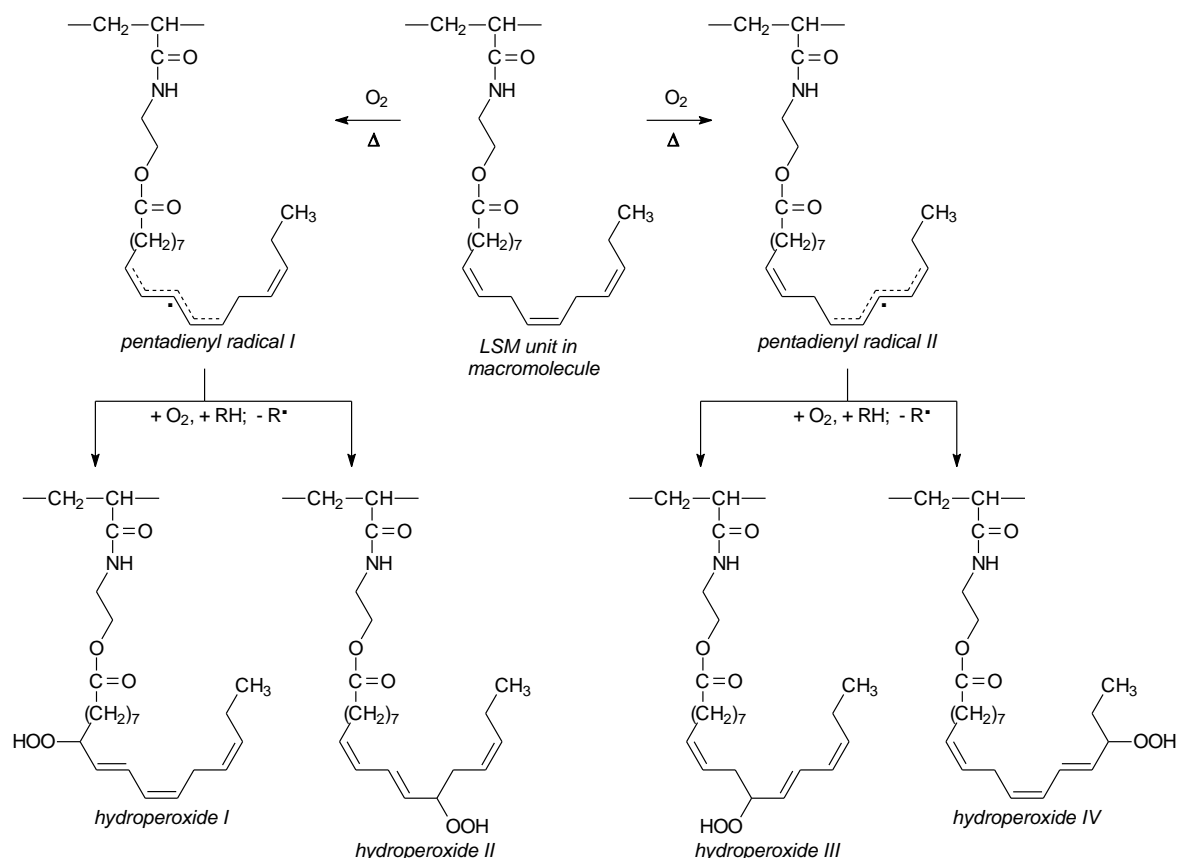
#### 342 4. Preparation of Polymeric Coatings from Plant Oil-Based Monomers

343 As shown by Solomon [30], both crude and modified plant oils are common film-forming  
344 materials for the production of paints and varnishes. Despite the emergence of various synthetic  
345 polymers based on vinyl and acrylic monomers, crude plant oils are still the basis of some paints for  
346 painting the roofs of houses and other outdoor objects. One of the disadvantages of such materials is  
347 the slow drying and relatively low moisture resistance. The synthesis of plant oil-based acrylic  
348 monomers opens new avenues for producing homo- and copolymers thereof with adjustable  
349 physical and mechanical properties (*e.g.*, flexibility, strength, *etc.*) due to formation of  
350 three-dimensional networks with controlled cross-linking density. The development of such  
351 coatings was shown to be carried out through oxidative cross-linking of the polymer network [31].

352 It should be noted that upon POBM application for the synthesis of latex polymers as highly  
353 hydrophobic film-forming protective coatings, they form three-dimensional networks with  
354 adjustable cross-linking density through the oxidative cross-linking mechanism.

355 Triglycerides of linseed oil contain about 52% of linolenic (*cis,cis,cis*-9,12,15-octadecatrienoic)  
356 acid chains which have three isolated carbon-carbon double bonds in their structure (Figure 10).  
357 Other fatty acids in linseed oil are oleic (*cis*-9-octadecenoic, 22%) and linoleic  
358 (*cis,cis*-9,12-octadecadienoic, 16%) acids. Hence, linolenate is a major constituent of LSM.

359 **Oxidative cross-linking** of the LSM-based copolymers is a free radical chain process consisting  
360 of chain initiation, propagation, and termination steps. Initiation, *i.e.* the formation of a fatty acid  
361 chain radical, can occur by thermal homolytic cleavage of a C–H bond or by a hydrogen atom  
362 abstraction from C–H by an initiator free radical. The bond dissociation energy of a bisallylic  
363 hydrogen is approximately 42 kJ/mol lower than that of an allylic hydrogen. As a result, linoleates  
364 and linolenates are more readily autooxidized and cross-linked in comparison with oleates.



365

366

367

**Figure 10.** Formation of radicals and hydroperoxides during oxidative cross-linking of polymers from linseed oil-based monomer (LSM).

368

369

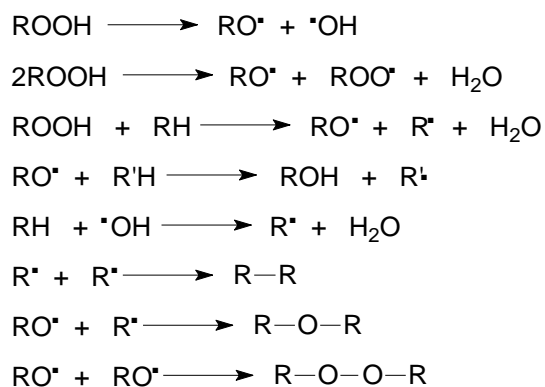
370

371

372

373

Hydrogen atom abstraction from C-11 or C-13 of the linolenate moiety leads to pentadienyl radicals I and II (Figure 10). Subsequent oxygen addition to radicals I and II generates peroxy radicals which are able of abstracting a hydrogen atom from a donor such as another linolenate moiety to form conjugated *trans,cis*-hydroperoxides I-IV (Figure 10). The hydroperoxides undergo decomposition reaction (Figure 11). The last three reactions lead to cross-linking of the macromolecules and formation of a polymer network.



374

375

where  $RH$  and  $R'H$  are unaltered fatty acid chains in macromolecules

**Figure 11.** Oxidative cross-linking of polymers from linseed oil-based monomer (LSM).

376

377

378

379

The main mechanical characteristics of films from latex polymers based on styrene or methyl methacrylate and the POBMs were determined. The composition of the copolymers was calculated from the  $^1H$  NMR spectroscopy data. The content of the olive and soybean monomers in the reaction mixture varied from 10 to 40 wt. % for copolymers with methyl methacrylate and from 25 to 60 wt. %

380 for copolymers with styrene. A plasticizing effect and enhanced hydrophobicity were observed for  
381 the copolymers synthesized from 2-N-acryloylaminoethyl oleate and 2-N-acryloylaminoethyl  
382 linoleate as comonomers. The unsaturation degree of the olive and soybean monomers was used as  
383 an experimental parameter to control the latex properties. The effect of monomer unsaturation on  
384 the cross-linking density of the latex films and, thus, on the physical and mechanical properties of  
385 the coatings was demonstrated [31].

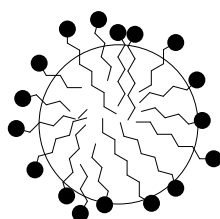
386 The decrease in the glass transition temperature of the latex copolymers (from 105 to 57°C for  
387 the copolymers of the olive and soybean monomers with methyl methacrylate and from 100 to 5°C  
388 for the copolymers with styrene) indicates that the presence of the OVM and SBM units in the  
389 macromolecules affects thermomechanical properties of the resulting latex copolymers. The olive  
390 and soybean monomer units impart flexibility to the macromolecules, improve the conditions of film  
391 formation, increase the strength in comparison with conventional polystyrene and poly(methyl  
392 methacrylate). Moreover, the OVM and SBM units in the macromolecules increase the  
393 hydrophobicity of polymeric latex films thus reducing the negative impact of water on the  
394 properties of the coatings.

395 Therefore, the incorporation of the hydrophobic fatty acid chains into the macromolecules of  
396 latex polymers allows for formation of polymer networks with a controlled cross-linking density  
397 along with enhancing the water resistance of the coatings. The copolymers based on the olive and  
398 soybean monomers enable the formation of coatings with low surface energy and water-repellent  
399 properties.

## 400 5. Formation of Micelles from the Complexes of Highly Hydrophobic Plant Oil-Based Monomers 401 with Sodium Dodecyl Sulfate

402 The synthesized POBMs contain  $\text{CH}_2=\text{CH}-\text{C}(\text{O})-\text{NH}-\text{CH}_2\text{CH}_2-\text{O}-\text{C}(\text{O})-$  as a hydrophilic  
403 fragment in their chemical structure and R- as a hydrophobic constituent in the fatty acid chain.  
404 Such a monomer structure imparts unique properties to the POBMs associated with the ability to  
405 participate in intermolecular (electrostatic and/or van der Waals) interactions to produce complexes  
406 (aggregates). The formed complexes can open up new opportunities for micellization and, thus, new  
407 approaches to conducting heterophase polymerization (*e.g.*, conventional emulsion and mini-  
408 emulsion polymerization).

409 The effect of highly hydrophobic olive oil-based and high oleic soybean oil-based (HO-SBM)  
410 acrylic monomers on micellization of sodium dodecyl sulfate (SDS) was examined at different  
411 surfactant and monomer concentrations by determining micellar parameters, size and structure, as  
412 well as surface tension measurements. The obtained results indicate SDS ability to solubilize  
413 sparingly soluble in water plant oil-based monomer molecules and facilitate formation of mixed  
414 (SDS/POBM) micelles (Figure 12). Surface activity of a surfactant/monomer mixture varies by  
415 adding the POBM and is generally higher than for SDS [32]. Comprehensive trends were observed  
416 for micellar aggregation number and number of micelle-bound monomer molecules demonstrating  
417 that POBM molecules replace SDS counterparts in the mixed micelles. Based on the dynamic light  
418 scattering measurements, it was hypothesized that incorporation of POBM into the mixed micelles  
419 promotes micellar association and formation of 25–30 nm size structures, also detected using  
420 transmission electron microscopy. Practical importance of these findings is the fact that  
421 solubilization of POBM by surfactant molecules can have an impact on reaction kinetics and  
422 mechanism of emulsion polymerization, as well as affect latex particles formation and, respectively,  
423 resulting particle morphology.



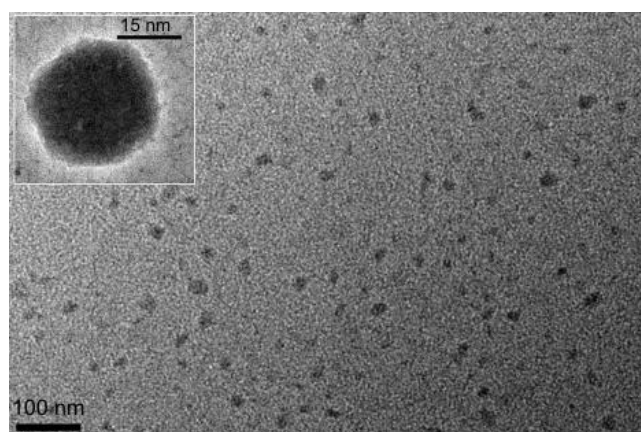
425 **Figure 12.** Possible location of the polar “heads” in a direct micelle from the SDS molecules and the  
 426 POBM/SDS aggregate.

427 Surfactants form direct micelles due to the interactions between hydrocarbon parts of their  
 428 molecules. Usually the micelle has a layered structure depending on the packaging of surfactant  
 429 molecules. A micelle contains a hydrocarbon nucleus, a water-hydrocarbon layer, which includes  
 430 2–3 methylene groups, and a layer of hydrated polar groups. It should be noted that surfactant  
 431 molecules are freely localized in the micelle. They can leave the micelle or move to a different  
 432 position; they can even be engulfed into the nucleus, which is determined by the hydrophobicity of  
 433 the surfactant fragment [33,34].

434 The feature of micellization of sodium dodecyl sulfate (SDS) in the presence of the plant  
 435 oil-based monomers is SDS ability to solubilize sparingly soluble in water POBM molecules and  
 436 facilitate formation of mixed (SDS/POBM) micelles. As shown by Kingsley et al. [32], the packing of  
 437 surface-active SDS/POBM complexes (aggregates) and the SDS molecules occurs upon micellization.  
 438 In this event, the SDS molecules can be squeezed out of the micelle and localized at the interphase  
 439 reducing the interfacial tension. Sodium dodecyl sulfate is known to have a micelle aggregation  
 440 number of 60–70 [34]. It was found that the aggregation number decreases to 10–48 (Table 3) upon  
 441 micellization of the SDS/POBM complexes. The micellar size depends on the packaging of the  
 442 surfactants. Their length and packing density in the micelle determine the radius of the hydrocarbon  
 443 nucleus. The formed colloidal solution simultaneously contains the SDS micelles and the mixed  
 444 SDS/POBM micelles. It should be noted that their size is 18–38 nm (Table 3, Figure 13) whereas the  
 445 SDS micellar size is 1.7–3.1 nm.

446 **Table 3.** Micellar parameters for SDS and POBM at different concentrations.

SDS + POBM (x,mol : y,mol)	$N_{agg}$	$N_{POBM}$	$I_1/I_3$	d,nm	PDI	$\sigma$ , mN/m
SDS at 0.02 M	41	0	1.04	3.1	0.006	36.2
+ HO-SBM 0.01 M	25	20	0.94	18.2	0.02	34.1
0.02 M	15	25	0.94	23.3	0.05	31.2
0.04 M	12	39	0.92	25.4	0.04	30.4
SDS at 0.05 M	57	0	1.03	1.7	0.003	34.9
+ HO-SBM 0.02 M	46	22	0.96	27.3	0.03	31.5
0.04 M	38	34	0.95	28.5	0.05	29.8
SDS at 0.02 M	41	0	1.03	3.1	0.006	36.2
+ OVM 0.01 M	27	22	0.95	22.6	0.06	32.4
0.02 M	19	31	0.93	28.7	0.04	31.1
0.04 M	10	33	0.93	37.8	0.04	30.1
SDS at 0.05 M	57	0	1.03	1.7	0.003	34.9
+OVM 0.02 M	48	23	0.95	28.2	0.02	32.6
0.04 M	31	28	0.94	33.9	0.04	30.2



447

448 **Figure 13.** TEM micrograph of micelles prepared by mixing SDS (0.02M) and HO-SBM (0.01M) (inset  
 449 shows morphology of selected individual micelle). Reprinted from Ref. 32, Copyright (2019), with  
 450 permission from Elsevier.

451 If the fatty acid chain cannot leave the hydrocarbon nucleus, the polar group can be even drawn  
 452 into the hydrophobic nucleus [34], which also affects the aggregation number. The authors explain  
 453 the features of micellization (micellar parameters, size, structure, and surface tension) and the  
 454 obtained results with the formation of surface-active SDS/POBM complexes (aggregates) of the  
 455 following structure (Figure 14):



456 **Figure 14.** Chemical structure of plant oil-based monomer (A), surfactant (B) and schematic of POBM  
 457 solubilization by SDS molecules (C). Reprinted from Ref. 32, Copyright (2019), with permission from  
 458 Elsevier.  
 459

460 The formation of a water-hydrocarbon layer of the spherical micelle leads to the localization of  
 461 the acrylic groups of the POBM molecule at the interface. This opens up new possibilities for the  
 462 formation of “core-shell” morphology, providing ability of POBM to undergo polymerization.

463 Chemical composition of plant oil-based monomer and SDS molecules is similar. They both  
 464 have polar “head” and long hydrophobic “tail” with in average 17 (POBM) and 12 (SDS) carbon  
 465 atoms. The obtained results indicate that SDS molecules solubilize sparingly soluble in water plant  
 466 oil-based monomer (POBM) counterparts, thus facilitating formation of mixed (SDS/POBM)  
 467 micelles. It was assumed that intermolecular interactions occur through physical association of both  
 468 molecular “heads” and “tails” in water. The data show that surface activity of a surfactant/monomer  
 469 mixture is generally higher than for SDS and varies by adding the POBM. Additionally, micellar  
 470 parameters, size and structure, observed changes upon the addition of POBM.

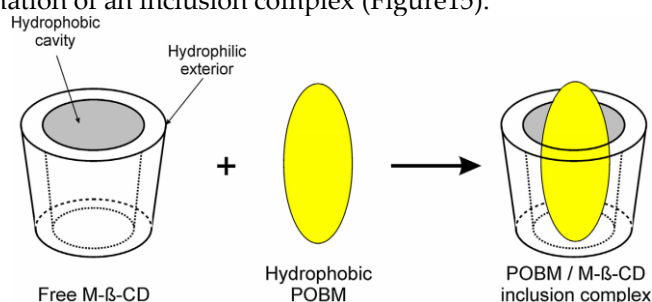
## 471 6. Dual Role of Methyl- $\beta$ -Cyclodextrin in the Emulsion Polymerization of Highly Hydrophobic 472 Plant Oil-Based Monomers

473 The new acrylic monomers are also capable of complexation with cyclodextrins, which play a  
 474 dual role in both enhancing POBM polymerizability as well as protecting against allylic termination  
 475 chain transfer.

476 Amphiphilic oligosaccharide, methyl- $\beta$ -cyclodextrin (M- $\beta$ -CD), was used to improve the  
 477 polymerizability of monomers from high oleic soybean and linseed oil in copolymerization with  
 478 styrene. Using X-ray diffractometry and differential scanning calorimetry, interactions between the  
 479 monomers and M- $\beta$ -CD were confirmed, while the formation of 1:1 complex from oligosaccharide  
 480 and each monomer molecules was demonstrated by mass spectrometry. In the presence of  
 481 “host-guest” complexes, polymer yield increases as the coagulum amount drops during the  
 482 emulsion polymerization of both plant oil-based monomers with styrene indicating their enhanced  
 483 aqueous solubility. Remarkably, latex polymers with a consistently higher molecular weight were  
 484 obtained in the presence of M- $\beta$ -CD. The complex formation and incorporation of monomer  
 485 molecules into the oligosaccharide cavities protect the fatty acid moieties and diminishes chain  
 486 transfer. The latter assumption was quantitatively confirmed in  $^1\text{H}$  NMR spectroscopy by  
 487 determining the number of protons of the alkyl carbon-carbon double bonds ( $-\text{CH}=\text{CH}-$ ) and the  
 488 bisallylic hydrogen atoms ( $-\text{CH}=\text{CH}-\text{CH}_2-\text{CH}=\text{CH}-$ ) in the unsaturated fatty acid moieties of the  
 489 latex copolymers. The observed effect is more pronounced for more unsaturated monomer from

490 linseed oil. Based on the obtained results, M- $\beta$ -CD plays a dual role in both enhancing POBM  
 491 polymerizability as well as protecting against allylic termination chain transfer.

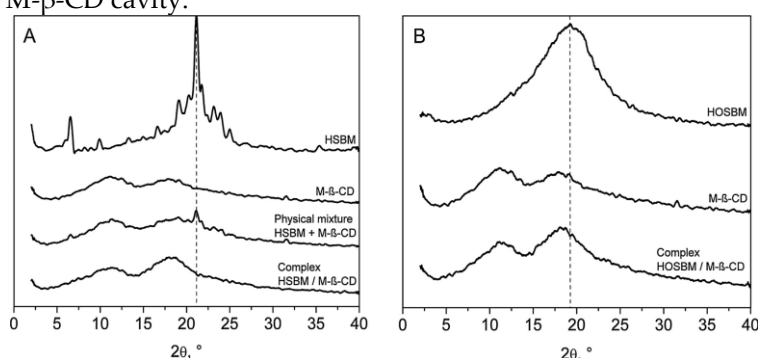
492 These results are explained by the specific structures of M- $\beta$ -CD having a hydrophobic cavity  
 493 and a hydrophilic exterior, and the POBM molecule, possessing a long hydrophobic fatty acid chain;  
 494 this results in the formation of an inclusion complex (Figure15).



495

496 **Figure 15.** Schematic illustration of the association of free methyl- $\beta$ -cyclodextrin and POBM to form a  
 497 1:1 inclusion complex. Reprinted from Ref. 35, Copyright (2018), with permission from Elsevier.

498 To confirm the formation of the inclusion complex, it was used Powder X-ray diffractometry  
 499 (PXRD) which is a powerful technique to detect the cyclodextrin complexation of small molecules in  
 500 a powder or crystalline state [36]. PXRD differentiates the formation of complexes due to clear  
 501 alterations between the diffraction pattern superposition of the components and the diffraction  
 502 pattern of the inclusion complex. The PXRD spectra of HSBM [monomer from hydrogenated (very  
 503 low degree of unsaturation) soybean oil], M- $\beta$ -CD, H-SBM/M- $\beta$ -CD inclusion complex, and the  
 504 physical mixture are shown in Figure 16A. The diffractogram of H-SBM displays numerous  
 505 characteristic peaks due to its self-lattice arrangement, which indicates the crystallinity of the  
 506 monomer. In contrast, M- $\beta$ -CD is an amorphous substance thus its diffractogram shows two wide  
 507 peaks related to the non-crystalline form. The diffraction pattern of the physical mixture of H-SBM  
 508 and M- $\beta$ -CD was just the superposition of the monomer and M- $\beta$ -CD. This may indicate that there is  
 509 no interaction between H-SBM and M- $\beta$ -CD in the simple physical mixture [37]. Compared with the  
 510 diffractogram of pure H-SBM and M- $\beta$ -CD, the diffraction pattern of the inclusion complex is similar  
 511 to that of the M- $\beta$ -CD with increased intensity of the peak at 17.9° at 2 $\theta$  scale and showed no  
 512 characteristic peaks that pure HS-BM had. These results indicate that the self-lattice arrangement of  
 513 H-SBM was changed from a crystalline to amorphous state, which can be attributed to the H-SBM  
 514 inclusion into the M- $\beta$ -CD cavity.



515

516 **Figure 16.** PXRD spectra of POBMs, methyl- $\beta$ -cyclodextrin, their physical mixture and inclusion  
 517 complexes (A – H-SBM, B – HO-SBM). Reprinted from Ref. 35, Copyright (2018), with permission  
 518 from Elsevier.

519 The PXRD pattern of HO-SBM, M- $\beta$ -CD, and HO-SBM/M- $\beta$ -CD inclusion complex are  
 520 presented in Figure 16B. HO-SBM is an oily viscous substance, and its diffractogram displays two  
 521 wide peaks attributed to the non-crystalline form. Since both M- $\beta$ -CD and HO-SBM are  
 522 non-crystalline substances, the formation of HO-SBM/M- $\beta$ -CD inclusion complex cannot be  
 523 confirmed unambiguously by PXRD.

524 The inclusion of a guest molecule into a cyclodextrin can also be studied using differential  
525 scanning calorimetry, as cavity alters the boiling and melting points of the initial substances by  
526 shifting or suppressing them [38]. The DSC thermograms of H-SBM, M- $\beta$ -CD, H-SBM/M- $\beta$ -CD  
527 inclusion complex, and the physical mixture are shown in Figure 17. The DSC curve of H-SBM  
528 shows two sharp endothermic peaks corresponding to the melting of the monomer. The DSC  
529 thermogram of M- $\beta$ -CD shows a broad endothermic band at 110°C due to the dehydration process.  
530 The endothermic peaks of H-SBM were observed in the thermogram of the physical mixture of  
531 H-SBM and M- $\beta$ -CD. These results indicate that the complexation has not occurred, and the initial  
532 substances are simply mixed together. However, no peak in the melting range of H-SBM was  
533 detected in the DSC curve of H-SBM/M- $\beta$ -CD samples prepared using the thin films method. This  
534 indicates that the monomer molecules are completely included into the M- $\beta$ -CD cavities, monomer  
535 appears in an amorphous state, and H-SBM/M- $\beta$ -CD inclusion complex forms.

536 The DSC thermogram of HO-SBM (data not shown) exhibited an endothermic peak at around  
537 17°C corresponding to the melting point of the monomer. However, no peak in the melting range of  
538 HO-SBM was detected in the DSC curves of HO-SBM/M- $\beta$ -CD inclusion complex and their physical  
539 mixture. This may imply that there was some interaction between the pure components. A plausible  
540 explanation is that unlike HSBM, HO-SBM is an oily liquid and, thus, monomer molecules might be  
541 able to penetrate into the M- $\beta$ -CD cavities when the two substances are mixed together. In principle,  
542 this procedure is similar to the kneading method, which is used for the synthesis of  
543 cyclodextrin-guest complexes when a liquid guest component is added to a slurry of cyclodextrin  
544 and kneaded thoroughly in a mortar [39].

545 Although PXRD and DSC analyses indicate the changes from a crystalline to amorphous state  
546 of H-SBM upon its interaction with M- $\beta$ -CD, these techniques can neither unambiguously confirm  
547 whether inclusion complexation (especially, for HO-SBM) occurs nor determine the complex  
548 stoichiometry. To this end, electrospray ionization–mass spectrometry (ESI–MS), which is an  
549 extremely sensitive and specific analytical technique, capable of providing the molecular masses  
550 within a sample and determination of molecular association of non-covalent bonding [39], was used  
551 in this work to monitor the formation of POBM/M- $\beta$ -CD inclusion complexes. The feasibility of ESI  
552 to maintain the non-covalent structure upon the transition of inclusion complexes from the liquid to  
553 gas phase has been widely applied to investigate the complexation of cyclodextrins with various  
554 organic substances [40].

555 Figure 17 shows the ESI mass spectra of inclusion complexes of the POBMs with  
556 methyl- $\beta$ -cyclodextrin. In the spectrum of H-SBM/M- $\beta$ -CD (Figure 17A), ions detected at  $m/z$  1665,  
557 1679, 1693, 1707, and 1721 correspond to sodium adducts of complexes of stearate-H-SBM with  
558 M- $\beta$ -CD having 9, 10, 11, 12, and 13 methyl groups, respectively. The ESI mass spectrum of the  
559 HO-SBM/M- $\beta$ -CD inclusion complex is depicted in Figure 17B. Ions that correspond to the inclusion  
560 of oleate-HO-SBM by M<sub>10-13</sub>- $\beta$ -CD (sodium adducts) are detected at  $m/z$  1677, 1691, 1705, and 1719. It  
561 is worth noting that stearate-H-SBM and oleate-HO-SBM are the main components of H-SBM and  
562 HO-SBM, respectively; M- $\beta$ -CD is a mixture of  $\beta$ -cyclodextrins in which 9–13 hydroxyl groups are  
563 substituted with methyl groups. For that reason, these above-mentioned inclusion complexes are the  
564 most pronounced in the ESI spectra.

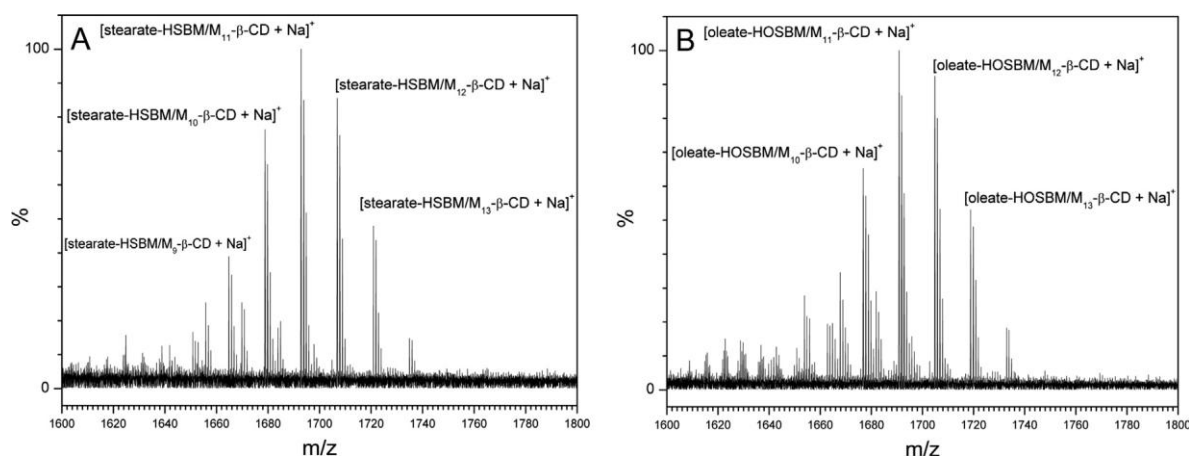


**Figure 17.** ESI mass spectra of H-SBM/M- $\beta$ -CD (A) and HO-SBM/M- $\beta$ -CD (B) inclusion complexes. Reprinted from Ref. 35, Copyright (2018), with permission from Elsevier.

Hence, the ESI-MS data directly confirmed the methyl- $\beta$ -cyclodextrin complexation of POBM molecules (both H-SBM and HO-SBM) resulting in the 1:1 complex formation (Figure 15).

It was shown that the emulsion copolymerization of POBMs with styrene in the presence of M- $\beta$ -CD allows for the protection and preservation of both fatty acid double bonds ( $-\text{CH}=\text{CH}-$ ) of the monomers and the bisallylic hydrogen atoms ( $-\text{CH}=\text{CH}-\text{CH}_2-\text{CH}=\text{CH}-$ ) in the case of latex polymers from LSM and styrene and fatty acid double bonds when HO-SBM is copolymerized with styrene. These results are consistent with previous reported literature on the cyclodextrin complexation of unsaturated fatty acids, reflecting protection of the latter against oxidation even in pure oxygen [41] due to burying the fatty acid double bonds into the CD cavity [42]. Thus, in the presence of M- $\beta$ -CD, the latex polymers with a consistently higher molecular weight can be obtained evidently because of the incorporation of POBM molecules into the M- $\beta$ -CD cavities that protects the fatty acid moieties and therefore decreases the chain transfer and addition of the fatty acid double bonds to growing radicals.

Furthermore, in the presence of M- $\beta$ -CD during the emulsion polymerization, the polymer yield increases and the coagulum amount decreases. The obtained data imply the dual role of M- $\beta$ -CD in the emulsion polymerization of POBMs, that is the enhanced aqueous solubility of highly hydrophobic monomers and their availability for the emulsion process as well as diminishing monomer chain transfer reactions due to “host-guest” complex formation.

A series of latexes from high oleic soybean- and linseed oil-based monomers was synthesized using emulsion copolymerization with styrene. In the presence of methyl- $\beta$ -cyclodextrin, latex polymers with a consistently higher molecular weight were obtained from both HO-SBM and LSM (this effect is more pronounced for more unsaturated LSM). Moreover, the emulsion copolymerization adding M- $\beta$ -CD resulted in an increased polymer yield and latex solid content accompanied by reduced coagulum formation. It was hypothesized that the incorporation of POBM molecules into the methyl- $\beta$ -cyclodextrin cavity diminishes the chain transfer contribution by protecting the allylic moiety of the POBM fatty acid fragments and simultaneously enhances the aqueous solubility and availability of POBMs in the emulsion polymerization process. Consequently, a higher molecular weight of latex polymers from highly hydrophobic POBMs can be obtained with higher monomer conversion and lower coagulum formation.

## 7. Conclusions

Monomers based on various plant oils were synthesized through a two-step procedure. A one-step process for the synthesis of new vinyl monomers by the reaction of direct transesterification of plant oil triglycerides with N-(hydroxyethyl)acrylamide was recently patented. The features of **homopolymerization** kinetics for the POBMs were determined. The reactivity of the plant oil-based monomers was studied by radical **copolymerization** with vinyl monomers. The Alfrey-Price Q (0.41–0.51) and e (0.09–0.28) parameters are close for all POBMs and do not essentially depend on

604 the monomer structure. The unique molecular structure of the plant oil-based acrylic monomers is  
605 that they simultaneously have a  $\text{CH}_2=\text{CH}-\text{C}(\text{O})-\text{NH}-\text{CH}_2\text{CH}_2-\text{O}-\text{C}(\text{O})-$  polar (hydrophilic)  
606 fragment capable of electrostatic interactions and a hydrophobic fatty acid chain (C15–C17) capable  
607 of van der Waals interactions. This opens up new opportunities for formation of micelles from the  
608 complexes of highly hydrophobic plant oil-based monomers with sodium dodecyl sulfate and new  
609 approaches to conducting heterophase polymerization.

610 Preparation of polymeric coatings from the plant oil-based monomers through the  
611 incorporation of the hydrophobic fatty acid chains into the macromolecules of latex polymers allows  
612 for formation of polymer networks with a controlled cross-linking density along with enhancing the  
613 water resistance of the coatings. The copolymers based on the olive and soybean monomers enable  
614 the formation of coatings with low surface energy and water-repellent properties. The copolymers  
615 based on the olive and soybean monomers enable the formation of coatings with low surface energy  
616 and water-repellent properties.

617 The formation of inclusion complexes upon the interaction between the molecules of the plant  
618 oil-based acrylic monomers and methyl- $\beta$ -cyclodextrin leads to a higher molecular weight of latex  
619 polymers from highly hydrophobic POBMs with higher monomer conversion and lower coagulum  
620 formation.

621 An analysis of the literature shows a rapid development of a new branch in polymer science  
622 related to the chemistry of aliphatic and aromatic biobased monomers from renewable plant sources.  
623 The synthesis of such monomers allows for producing fully biobased polymers with biocompatible  
624 and biodegradable properties which do not pollute the environment. Copolymerization of the  
625 biobased monomers with commercial monomers enables formation of copolymers with controlled  
626 physical, chemical, and mechanical properties.

## 627 8. Patents

628 Biobased Acrylic Monomers US 10,315,985 B2 June 11<sup>th</sup>, 2019.

629 Biobased Acrylic Monomers and Polymers Thereof US 10,584,094 B2 March 10<sup>th</sup>, 2020.

630 **Author Contributions:** Conceptualization, A.K., S.V. and A.V.; methodology, Z.D., V.K., K.K. and O.S.;  
631 investigation, A.K., Z.D., V.K., K.K. and O.S.; writing—original draft preparation, A.K., V.K. and S.V.;  
632 writing—review and editing, S.C. and A.V.; project administration, S.C. and A.V.; funding acquisition, A.V. All  
633 authors have read and agreed to the published version of the manuscript.

634 **Funding:** ND EPSCoR RII Track 1 ((IIA-1355466), North Dakota Department of Commerce, North Dakota  
635 Department of Agriculture, United Soybean Board.

636 **Conflicts of Interest:** The authors declare no conflict of interest. The funders had no role in the design of the  
637 study; in the collection, analyses, or interpretation of data; in the writing of the manuscript, or in the decision to  
638 publish the results.

639

640 **References**

- 641 1. Papageorgiou, G.Z. Thinking Green: Sustainable Polymers from Renewable Resources. *Polymers* **2018**, *10*,  
642 952.
- 643 2. Sharmin, E.; Zafar, F.; Akram, D.; Alam, M.; Ahmad, S. Recent advances in vegetable oils based  
644 environment friendly coatings: A review. *Ind. Crops Prod.* **2015**, *76*, 215–229.
- 645 3. Xia, Y.; Larock, R.C. Vegetable oil-based polymeric materials: Synthesis, properties, and applications.  
646 *Green Chem.*, **2010**, *12*, 1893–1909.
- 647 4. Can, E.; Wool, R.P.; Kusefoglu, S. Soybean- and Castor-oil-based thermosetting polymers: Mechanical  
648 properties. *J. Appl. Polym. Sci.* **2006**, *102*, 1497–1504.
- 649 5. Van De Mark, M.R.; Sandefur, K. Vegetable Oils in Paint and Coatings. In *Industrial Uses of Vegetable Oils*,  
650 Erhan, S.Z., Ed.; AOCs Press: Boca Raton, FL, United States, 2005; pp. 149–168.
- 651 6. Statista. Available online:  
652 <https://www.statista.com/statistics/263933/production-of-vegetable-oils-worldwide-since-2000/> (accessed  
653 on 25<sup>th</sup> of May, 2020).
- 654 7. Moreno, M.; Miranda, J.I.; Goikoetxea, M.; Barandiaran, M. Sustainable polymer latexes based on linoleic  
655 acid for coatings applications. *Prog. Org. Coat.* **2014**, *77*, 1709–1714.
- 656 8. Yuan, L.; Wang, Z.; Trenor, N.M.; Tang, C. Amidation of triglycerides by amino alcohols and their impact  
657 on plant oil-derived polymers. *Polym. Chem.* **2016**, *7*, 2790–2798.
- 658 9. Moreno, M.; Lampard, Ch.; Williams, N.; Lago, E.; Emmett, S.; Goikoetxea, M.; Barandiaran, M.J.  
659 Eco-paints from bio-based fatty acid derivative latexes. *Prog. Org. Coat.* **2015**, *81*, 101–106.
- 660 10. Tarnavchyk, I.; Popadyuk, A.; Popadyuk, N.; Voronov, A. Synthesis and Free Radical Copolymerization of  
661 a Vinyl Monomer from Soybean Oil. *ACS Sustain. Chem. Eng.* **2015**, *3*, 1618–1622.
- 662 11. Demchuk, Z.; Shevchuk, O.; Tarnavchyk, I.; Kirianchuk, V.; Kohut, A.; Voronov, S.; Voronov, A. Free  
663 Radical Polymerization Behavior of the Vinyl Monomers from Plant Oil Triglycerides. *ACS Sustain. Chem.*  
664 *Eng.* **2016**, *4*, 6974–6980.
- 665 12. Tarnavchyk, I.; Voronov, A. Biobased acrylic monomers - US 10,315,985 B2 June 11<sup>th</sup>, 2019.
- 666 13. Demchuk, Z.; Shevchuk, O.; Tarnavchyk, I.; Kirianchuk, V.; Lorenson, M.; Kohut, A.; Voronov, S.;  
667 Voronov, A. Free Radical Copolymerization Behavior of Plant Oil-Based Vinyl Monomers and Their  
668 Feasibility in Latex Synthesis. *ACS Omega* **2016**, *1*, 1374–1382.
- 669 14. Kingsley, K.; Shevchuk, O.; Kirianchuk, V.; Kohut, A.; Voronov, S.; Voronov, A. Emulsion  
670 Copolymerization of Vinyl Monomers from Soybean and Olive Oil: Effect of Counterpart Aqueous  
671 Solubility. *Eur. Polym. J.* **2019**, *119*, 239–246.
- 672 15. Harrison, S.A.; Wheeler, D.H. The Polymerization of Vinyl and Allyl Esters of Fatty Acids. *J. Am. Chem.*  
673 *Soc.* **1951**, *73*, 839–842.
- 674 16. Chen, F.B.; Bufkin, G. Crosslinkable Emulsion Polymers by Autoxidation. I. Reactivity Ratios. *J. Appl.*  
675 *Polym. Sci.* **1985**, *30*, 4571–4582.
- 676 17. Chen, F.B.; Bufkin, G. Crosslinkable Emulsion Polymers by Autoxidation. II. *J. Appl. Polym. Sci.* **1985**, *30*,  
677 4551–4570.
- 678 18. Boshui, C.; Nan, Z.; Jiang, W.; Jiu, W.; Jianhua, F.; Kai, L. Enhanced biodegradability and lubricity of  
679 mineral lubricating oil by fatty acidic diethanolamide borates. *Green Chem.* **2013**, *15*, 738–743.
- 680 19. Yuan, L.; Wang, Z.; Trenor, N.M.; Tang, C. Robust Amidation Transformation of Plant Oils into Fatty  
681 Derivatives for Sustainable Monomers and Polymers. *Macromolecules* **2015**, *48*, 1320–1328.
- 682 20. Chen, R. Bio-based polymeric materials from vegetable oils. PhD Thesis, Iowa State University, Ames, IA,  
683 United States, 2014.
- 684 21. Voirin, C.; Caillol, S.; Sadavarte, N.V.; Tawade, B.V.; Boutevin, B.; Wadgaonkar, P.P. Functionalization of  
685 cardanol: towards biobased polymers and additives. *Polym. Chem.* **2014**, *5*, 3142–3162.
- 686 22. Jailliet, F.; Darroman, E.; Boutevin, B.; Caillol, S. A chemical platform approach on cardanol oil: from the  
687 synthesis of building blocks to polymer synthesis. *OCL - Oilseeds and fats crops and lipids* **2016**, *23*, 511–518.
- 688 23. Demchuk, Z.; Li, W.S.J.; Eshete, H.; Caillol, S.; Voronov, A. Synergistic Effects of Cardanol- and High Oleic  
689 Soybean Oil Vinyl Monomers in Miniemulsion Polymers. *ACS Sustain. Chem. Eng.* **2019**, *7*, 9613–9621.
- 690 24. Mhadeshwar, N.; Wazarkar, K.; Sabnis, A.S. Synthesis and characterization of ricinoleic acid derived  
691 monomer and its application in aqueous emulsion and paints thereof. *Pigment & Resin Technology* **2019**, *48*,  
692 <https://doi.org/10.1108/PRT-09-2017-0078>.

- 693 25. Tarnavchuk, I.; Voronov, A. Biobased acrylic monomers and polymers thereof - US 10,584,094 B2  
694 March 10<sup>th</sup>, 2020.
- 695 26. Barison, A.; da Silva, C.W.; Campos, F.R.; Simonelli, F.; Lenz, C.A.; Ferreira, A.G. A simple methodology  
696 for the determination of fatty acid composition in edible oils through <sup>1</sup>H NMR spectroscopy. *Magn. Reson.*  
697 *Chem.* **2010**, *48*, 571–659.
- 698 27. Bozell, J.J. Feedstocks for the future – biorefinery production of chemicals from renewable carbon.  
699 *Clean–Soil, Air, Water* **2008**, *36*, 641–647.
- 700 28. Boskou, D. *Olive Oil Chemistry and Technology*, 2nd ed.; AOCS Publishing: New York, United States, 2006,  
701 288 p.
- 702 29. Kingsley, K.; Shevchuk, O.; Demchuk, Z.; Voronov, S.; Voronov, A. The features of emulsion  
703 copolymerization for plant oil-based vinyl monomers and styrene. *Ind. Crops Prod.* **2017**, *109*, 274–280.
- 704 30. Solomon, D.H. *The Chemistry of Organic Film Formers*, Robert E. Krieger Publishing Co.: Huntington, NY,  
705 United States, 1977; 412 p.
- 706 31. Demchuk, Z.; Kohut, A.; Voronov, S.; Voronov, A. Versatile Platform for Controlling Properties of Plant  
707 Oil-Based Latex Polymer Networks. *ACS Sustain. Chem. Eng.* **2018**, *6*, 2780–2786.
- 708 32. Kingsley, K.; Shevchuk, O.; Voronov, S.; Voronov, A. Effect of highly hydrophobic plant oil-based  
709 monomers on micellization of sodium dodecyl sulfate. *Colloids Surf. A Physicochem. Eng. Asp.* **2019**, *568*,  
710 157–163.
- 711 33. Mittal, K.L. *Micellization, Solubilization, and Microemulsions*, Vols. 1 and 2; Plenum: New York, United  
712 States, 1977; 487; 945 pp.
- 713 34. Rusanov, A.I. *Micellization in solutions of surfactants (in Russian)*; Khimiya: St. Petersburg, Russian  
714 Federation, 1992; 280 p.
- 715 35. Kohut, A.; Demchuk, Z.; Kingsley, K.; Voronov, S.; Voronov, A. Dual role of methyl- $\beta$ -cyclodextrin in the  
716 emulsion polymerization of highly hydrophobic plant oil-based monomers with various unsaturations.  
717 *Eur. Polym. J.* **2018**, *108*, 322–328.
- 718 36. Michalska, P.; Wojnicz, A.; Ruiz-Nuño, A.; Abril, S.; Buendia, I.; León, R. Inclusion complex of ITH12674  
719 with 2-hydroxypropyl- $\beta$ -cyclodextrin: Preparation, physical characterization and pharmacological effect.  
720 *Carbohydr. Polym.* **2017**, *157*, 94–104.
- 721 37. Liao, Y.; Zhang, X.; Li, C.; Huang, Y.; Lei, M.; Yan, M.; Zhou, Y.; Zhao, C. Inclusion complexes of  
722 HP- $\beta$ -cyclodextrin with agomelatine: Preparation, characterization, mechanism study and *in vivo*  
723 evaluation. *Carbohydr. Polym.* **2016**, *147*, 415–425.
- 724 38. Cabral Marques, H.M.; Hadgraft, J.; Kellaway, I.W. Studies of cyclodextrin inclusion complexes. I. The  
725 salbutamol-cyclodextrin complex as studied by phase solubility and DSC. *Int. J. Pharm.* **1990**, *63*, 259–266.
- 726 39. Guo, M.Q.; Song, F.; Zhiqiang, L.; Shuying, L. Characterization of non-covalent complexes of rutin with  
727 cyclodextrins by electrospray ionization tandem mass spectrometry. *J. Mass Spectrom.* **2004**, *39*, 594–599.
- 728 40. Marangoci, N.; Mares, M.; Sillion, M.; Fifere, A.; Varganici, C.; Nicolescu, A.; Deleanu, C.; Coroaba, A.;  
729 Pinteala, M.; Simionescu, B.C. Inclusion complex of a new propiconazole derivative with  $\beta$ -cyclodextrin:  
730 NMR, ESI-MS and preliminary pharmacological studies. *Results Pharma Sci.* **2011**, *1*, 27–37.
- 731 41. Szejtli, J.; Bánky-Elöd, E.I. Inclusion Complexes of Unsaturated Fatty Acids with Amylose and  
732 Cyclodextrin. *Starch* **1975**, *27*, 368–376.
- 733 42. Jyothirmayi, N.; Ramadoss, C.; Divakar, S. Nuclear magnetic resonance studies of cyclodextrin complexes  
734 of linoleic acid and arachidonic acid. *J. Agric. Food Chem.* **1991**, *39*, 2123–2127.



© 2020 by the authors. Submitted for possible open access publication under the terms and conditions of the Creative Commons Attribution (CC BY) license (<http://creativecommons.org/licenses/by/4.0/>).